PROCEEDINGS, Fourteenth Workshop on Geothermal Reservoir Engineering
Stanford University, Stanford, California, January 24-26, 1989
SGP-TR-122

FLUID CHEMISTRY AND HYDROLOGY OF THE HEBER GEOTHERMAL SYSTEM, CALIFORNIA

M.C. Adams(1), M. Lemieux(1), J.N. Moore(1), and S.D. Johnson(2)

1 University of Utah Research Institute, Salt Lake City, UT
2 Chevron Resources Company, San Ramon, CA

ABSTRACT

This paper presents the results of chemical and isotopic analyses of geothermal fluids and microthermometric measurements on fluid inclusions from the Heber geothermal system. The chemical analyses indicate that the reservoir fluids have salinities near 15000 ppm total dissolved solids and low gas contents. Small but consistent differences in the concentrations of total CO_2, B, Li, O-18, and deuterium are found between the fluids that feed the two power plants. These differences may be due to divergent paths of the thermal fluids as they flow from the south.

Fluid inclusion homogenization temperatures are similar to the present temperatures in a gradient well near the zone of upflow but are generally lower in the other two wells studied. Salinities determined from the freezing measurements suggest that the fluids contained within the inclusions are mixtures of the production fluids and other lower-salinity waters.

INTRODUCTION

The Salton Trough of southern California and Mexico is a major geothermal province hosting over a dozen separate thermal systems. With the exception of the geothermal system at Cerro Prieto (see, for example, Truesdell et al., 1981) few data have been published on the chemistry of the reservoir fluids that characterize this province. In this paper we present chemical and thermal data from the Heber geothermal system. These data were obtained from chemical analyses collected from production wells during 1987 and from microthermometric measurements on fluid inclusions contained within secondary calcite.

The Heber geothermal system is located 7 km north of the Mexico-U.S. border. The field currently has an installed capacity of 119 MW from a 52 MW dual flash plant (eastern production island) and a 67 MW binary plant (western production island). The location of the wells sampled in this study and the temperatures at a depth of 1830 m are shown in Figure 1. Based on the thermal data, James et al. (1987) concluded that an upwelling center is located near GTW 6, which has a bottom hole temperature of 199°C. They also concluded that fluid flow is to the north, towards the producing wells.

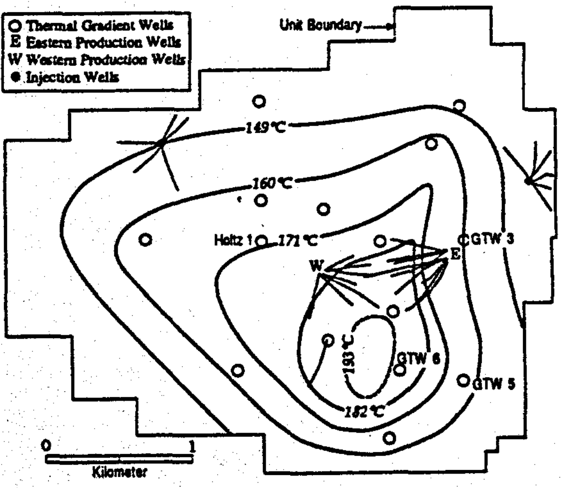

Figure 1. Location map of production, injection, and thermal gradient wells in the Heber geothermal field. Isotherms at a depth of 1830 m are also shown. Figure modified from James et al. (1987).

The geology and reservoir characteristics of the field have been described by Tansev and Wasserman (1978), Lippmann and Bovardsson (1985), and James et al. (1987). According to James et al. (1987), the geothermal system can be divided into three permeability units. These include the capping clays from 150 to 550 m, high matrix permeability sandstones from 550 to 1700 m, and permeable northwest- and northeast-trending fracture zones below 1700 m.

FLUID CHEMISTRY

Fluids from the eastern wells were sampled during August and December, 1987. The fluids were sampled primarily from sample ports on top of the flow-lines within ten feet of the wellhead. Although flow in these wells is two-phase, the phases were found to be stratified at the position of the ports. Stratification was confirmed by the chloride content and pH of fluids taken during vertical traverses through the pipe with a sampling probe. The liquid samples were taken with the vertical probe near the bottom of horizontal flowlines, where the chloride contents and pH were highest. The gas samples were taken directly from the top port using a mini-cyclone separator. Chemical analyses of the steam condensates consistently showed less than a few ppm of Cl, indicating that good separations of brine and steam were achieved.

Fluids from the western production island were sampled during eight-hour flow tests in December, 1987. Samples were taken every two hours from the weirbox and also at the end of each test period using a mini-cyclone separator.

The chemical compositions of the fluids prior to boiling were reconstructed from the gas and liquid analyses using steam fraction values derived from measured downhole temperatures (eastern wells) or wellhead temperatures (western wells). The recombined analyses are shown in Table 1. Examination of Table 1 shows that while the concentrations of Na, K, and Cl in all of the fluids sampled are very similar, concentrations of SO_4, the minor elements, total CO_2, 0-18, and deuterium display small but consistent differences between the two production islands.

The differences in the concentrations of the minor elements between the two production islands, particularly with respect to B, Li, and the stable isotopes, indicate that the western fluid has mixed with a small amount of lower-temperature fluid (see Table 1 and Fig. 2). In general, low temperature fluids exhibit lower B and Li, and lower isotope values.

Figures 3a and 3b show the variation of SO_4 and total CO_2 with respect to Ca. Because calcite scaling results in a loss of one mole of total CO_2 per mole of Ca, total CO_2 is plotted to preserve the relationship between these components. It can be seen that Ca varies directly with SO_4, but inversely with total CO_2. For a fluid in equilibrium with anhydrite and calcite, Ca, SO_4, and total CO_2 will increase as the temperature of the fluid decreases. The positive correlation of Ca with SO_4 and the higher concentrations of these elements in the western fluids suggest that the western fluids have equilibrated with anhydrite at a slightly lower temperature than the eastern fluids.

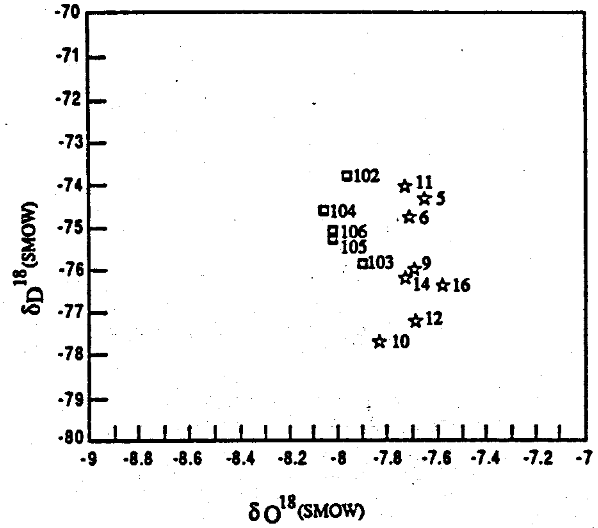

Figure 2. Isotopic compositions of the Heber geothermal fluids. The compositions are corrected for steam loss. The meteoric water line is to the left of the Heber compositions. Wells feeding the eastern production island are shown with stars and those feeding the western production island are shown with squares.

The inverse correlation between Ca and total CO_2 implies a mass-action relationship, where an increase in total CO_2 results in a decrease in Ca. As shown in Figure 3b, this relationship is well defined for the eastern fluids. The inverse correlation between these species thus implies that the elevated levels of CO_2 found in the eastern fluids resulted from either the addition of CO_2 or mixing with a CO_2-enriched fluid.

The differences in chemistry between the eastern and western fluids cannot be attributed to the depth of production because the wells all draw from similar depths. However, the wells do produce from different portions of the field. Figure 1 shows that the thermal contours at 1829 m are elongated along the fault that intersects the eastern wells. Thus the thermal fluid traveling northward from the vicinity of GTW 6 may diverge physically and chemically prior to reaching the western and eastern wells.

TABLE 1. Preflash chemical compositions of fluids from the Heber geothermal field. Chemical concentrations are in parts per million, isotopic concentrations are in per mil, and geothermometer temperatures (Fournier and Truesdell,1973; Fournier, 1981) are in degrees C. NA = not analyzed and AC = air contamination. Gas analyses were performed by Thermochem, Inc., chemical analyses by UURI, and isotopic analyses by SMU. Alk. = total alkalinity as HCO3.

WELL	DATE	Na	K	Ca	Mg	SiO2	B	Li	Sr	Ba
5	Dec-87	4019	333	750	1.76	237	4.12	6.64	40.6	4.39
6	Dec-87	4034	340	747	2.12	224	4.12	6.62	40.3	4.19
9	Dec-87	4060	332	717	2.05	243	4.17	6.75	41.1	4.64
10	Aug-87	4012	342	686	1.96	230	4.02	6.57	39.8	4.05
11	Dec-87	4242	354	655	2.81	221	4.25	6.92	45.4	4.22
12	Dec-87	4261	349	736	2.42	232	4.35	7.17	42.7	4.42
13	Aug-87	4140	324	565	2.31	275	4.83	7.89	45.2	4.98
14	Dec-87	4091	327	687	2.72	210	4.30	6.91	42.6	4.20
16	Dec-87	4147	317	617	3.42	207	4.82	7.90	46.0	4.73
101	Dec-87	3967	366	836	2.72	207	3.75	6.04	36.9	4.16
102	Dec-87	3925	347	816	1.83	208	3.64	5.67	35.7	3.83
103	Dec-87	3766	303	843	1.77	220	3.41	5.30	37.7	3.55
104	Dec-87	3840	338	810	1.79	206	3.60	5.53	35.5	3.78
105	Dec-87	3683	333	830	1.88	212	3.47	5.38	34.0	3.77
106	Dec-87	3907	359	794	1.60	212	3.67	5.84	35.3	3.95
107	Dec-87	3746	281	985	1.54	233	3.15	4.31	35.1	3.55
108	Dec-87	3908	329	839	1.19	249	3.59	5.47	36.6	4.30
110	Aug-87	3792	318	709	2.28	248	3.56	5.21	32.3	4.04

WELL	NH4	ALK.	Cl	F	SO4	TDS	Qtz Geoth.	Na-K-Ca Geoth.	Liq. Fract.	Steam Fract.
5	5.66	30.6	7758	2.04	65.9	13243	192	195	0.93	0.07
6	5.67	31.6	7738	2.79	63.2	13226	188	196	0.93	0.07
9	5.67	30.2	7815	2.01	64.0	13312	194	195	0.91	0.09
10	5.53	30.4	7746	2.30	73.7	13136	179	198	0.92	0.08
11	6.10	30.1	7835	1.82	62.9	13410	187	198	0.91	0.09
12	5.70	30.4	7866	2.02	64.4	13591	190	196	0.92	0.08
13	6.98	30.0	7625	3.49	59.7	13299	203	196	0.92	0.08
14	5.89	31.3	7801	2.03	59.9	13260	183	194	0.92	0.08
16	7.15	33.9	7758	2.20	55.0	13195	182	193	0.92	0.08
101	3.51	28.2	8105	2.22	77.8	13632	182	200	0.86	0.10
102	4.78	31.6	7667	2.16	74.0	13111	183	198	0.90	0.10
103	4.35	29.9	7429	2.17	83.4	12717	186	191	0.91	0.11
104	4.66	29.6	7571	2.15	74.5	12911	182	197	0.90	0.10
105	4.39	29.6	7598	2.06	71.7	12796	184	198	0.90	0.11
106	4.99	28.1	7673	2.63	66.2	13083	184	200	0.91	0.09
107	3.61	20.9	7318	4.10	100.0	12727	191	186	0.86	0.09
108	3.11	22.7	7871	2.69	73.9	13338	195	195	0.84	NA
110	3.78	57.1	7727	2.52	84.7	12960	193	197	0.84	NA

WELL	Delta O-18	Delta D	CO2	H2S	NH3	Ar	N2	CH4	H2
5	-7.65	-74.3	186	1.35	2.65	0.364	15.3	3.00	0.01368
6	-7.71	-74.7	197	1.47	2.76	0.381	14.1	2.72	0.00749
9	-7.69	-76.0	217	1.50	3.25	0.360	15.9	3.10	0.01677
10	-7.83	-77.7	207	1.70	2.92	0.359	14.9	2.80	0.01066
11	-7.73	-74.1	251	1.33	3.65	AC	AC	3.47	0.03213
12	-7.69	-77.2	212	1.30	3.16	AC	AC	3.33	0.01040
13	-7.69	-75.5	189	0.84	4.15	AC	AC	2.44	0.01911
14	-7.72	-76.2	238	1.11	3.16	0.453	17.4	3.65	0.02007
16	-7.59	-76.4	304	0.86	4.02	0.514	19.8	5.22	0.01992
101	NA	NA	230	2.27	2.63	0.576	21.6	3.31	0.06540
102	-7.96	-73.8	163	1.75	2.39	0.447	17.9	2.52	0.06311
103	-7.90	-75.7	127	1.11	2.14	0.369	14.6	2.23	0.03647
104	-8.06	-74.6	179	1.91	2.39	0.284	20.9	2.79	0.08621
105	-8.02	-75.3	163	1.34	2.63	AC	AC	2.82	0.02340
106	-8.02	-75.1	167	1.70	2.54	0.416	16.4	2.33	0.03301
107	NA	NA	145	1.35	1.81	0.497	19.2	2.05	0.10656

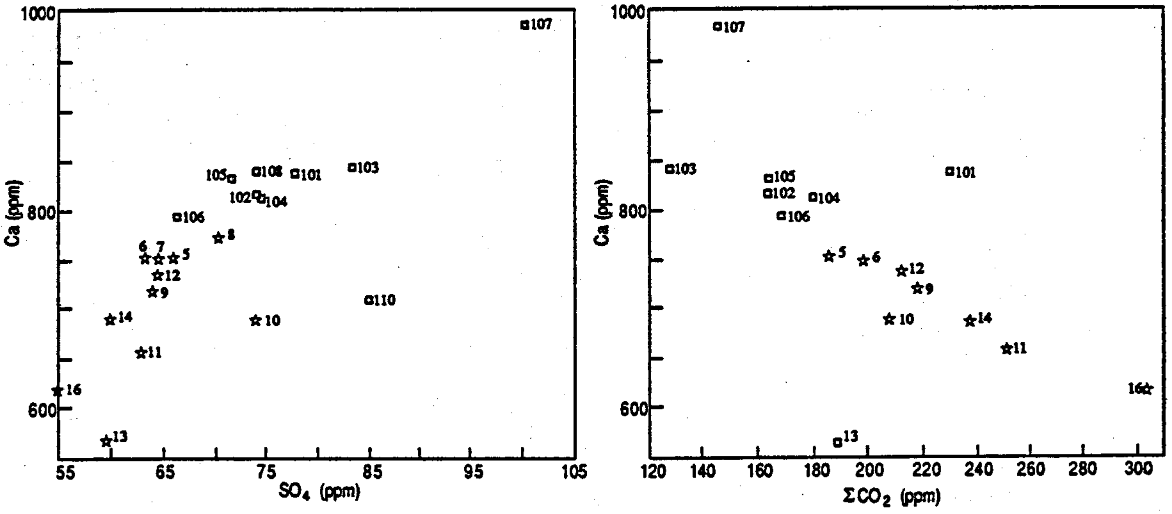

Figure 3. Variation of SO_4 and total CO_2 (HCO_3 + CO_2 in Table 1) with Ca in the Heber geothermal fluids. Note that the eastern production wells precipitate calcite in the wellbore. For an explanation of symbols see figure 2.

FLUID INCLUSION RESULTS

Calcite veins were sampled for fluid inclusions from wells GTW 3, GTW 5, and GTW 6 (Fig. 1). Veins ranging up to 2 mm in thickness are common within the shales below depths of 760 m in these wells.

All the fluid inclusions examined in this study were liquid-rich and contained a small vapor bubble that occupied about 15% of the inclusion volume at room temperature. Most of the inclusions studied are secondary or psuedosecondary, occurring along short, healed fractures within the interiors of the crystals.

Fluid inclusion heating and freezing measurements were made using a Fluid Inc. heating/freezing system. All measurements were made in duplicate. Replicate measurements were within 0.2°C. Most of the inclusions had maximum dimensions in the range of 2 to 15 microns. No evidence of a gas phase other than water or of daughter minerals were found in any of the inclusions.

The homogenization temperatures of the fluid inclusions from the three wells are plotted against depth in Figures 4a through 4c. For comparison, the measured downhole temperatures are also shown. Figures 4b and 4c show that the homogenization temperatures of inclusions in wells GTW 5 and 6 are similar and range from 130° to 202°C. Higher temperatures, reaching 244°C are recorded in fluid inclusions from GTW 3.

In many of the calcite crystals examined, two or three distinct generations of inclusions can be distinguished on the basis of their homogenization temperatures. For example, at 1820 m in GTW 5, three distinct generations are present. These are defined by homogenization temperatures ranging from 135°-140°C, 160°-165°C and 180°C. However, no cross-cutting relationships were observed which could be used to establish the relative ages of the different sets of inclusions. Browne (1977) also recognized two distinct thermal episodes in his study of Holtz 1 (refer to Fig. 1 for location).

Ice-melting temperatures range from -0.3° to -0.7°C in GTW 3, 0.0° to -0.8°C in GTW 5, and 0.0° to-0.6°C in GTW 6. For reference a freezing point depression of 0.8°C corresponds to a salinity of 1.4 equivalent weight percent NaCl (Potter et. al., 1978). No systematic differences in ice-melting temperatures were apparent with respect to depth or homogenization temperature.

Evidence for the formation of CO_2 clathrate during freezing was observed in inclusions from a depth of 1072 m in GTW 3. These inclusions displayed melting temperatures of +0.6°C, and initial freezing temperatures near -30°C. No other examples of CO_2-enriched fluids were observed.

DISCUSSION

The results of our chemical and fluid inclusion studies can be combined with the geologic studies of James et al. (1987) and the modeling study of Lippmann and Bovardsson

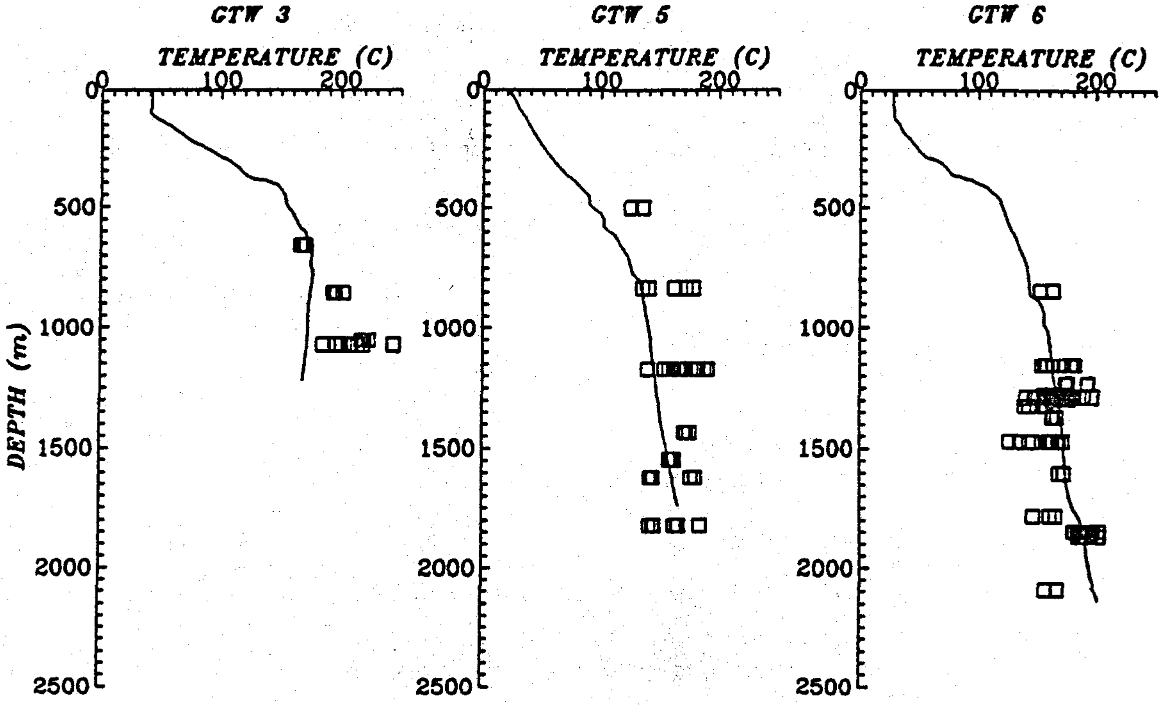

Figure 4. Fluid inclusion homogenization temperatures and measured temperatures in thermal gradient wells GTW 3, 5, and 6. The fluid inclusion temperatures are shown by squares and the measured temperatures by solid lines.

(1985) to refine the existing hydrogeochemical model of the geothermal system. The primary features of these previous studies are the presence of an upflow zone located to the south of GTW 6, a northward-trending thermal plume that feeds the production wells, and some recharge through the capping clays.

Our fluid inclusion studies of the wells near the upflow zone, GTW 5 and 6, suggest a complex pattern of heating and cooling within this region of the field. Comparison of Figures 4b and 4c shows that downhole measured temperatures are most similar to the lower limit of the fluid inclusion homogenization temperatures in GTW 5, but near the upper end of the homogenization temperatures in GTW 6. These relationships indicate that the rocks in GTW 5 are cooling whereas those in GTW 6 are being heated. Furthermore, maximum measured fluid inclusion temperatures in GTW 6 are approximately 20°C hotter than those in GTW 5 at similar depths. We infer from these observations that GTW 6 is closer to the source of the thermal plume than GTW 5, and that permeabilities in GTW 5 have been reduced since the inclusions formed.

The salinities of the fluid inclusions demonstrate that the upwelling fluids were diluted by lower-salinity waters. The maximum salinities of the fluid inclusions are similar to the 15000 ppm TDS contents of the produced fluids. However, the fluid inclusions also record salinities that range downward to less than 1700 ppm, indicating that significant mixing has occurred. The low-salinity fluids may in part represent meteoric water that has percolated through the clay cap, as proposed by Lippmann and Bovardsson (1985).

A small amount of mixing is also apparent in the chemistry of the fluids produced at the power plants, approximately 1.5 km north of GTW 6. Fluids that feed the western binary plant, which is slightly off-center of the thermal anomaly, display a minor amount of mixing and cooling. Fluids that feed the eastern dual flash plant have more CO_2 than the western fluids, indicating either an addition of CO_2 or mixing with CO_2-bearing fluids. CO_2-enriched fluids were also found in fluid inclusions at 1072 m in GTW 3, a thermal gradient well adjacent to the eastern production wells.

CONCLUSIONS

The fluids produced at the two production islands are slightly different in chemistry. The chemical compositions indicate that the fluids which feed the western binary plant may have mixed with another fluid and cooled slightly with respect to those that feed the eastern dual flash plant.

Our fluid inclusion studies are consistent with the geologic model of James et al. (1987), which indicates that the upwelling center is located in the southern part of the field. A comparison of the measured and fluid inclusion temperatures suggests that the rocks in GTW 5 are cooling. In contrast, the measured temperatures in GTW 6 are near the highest temperatures recorded by the fluid inclusions.

Chemical analyses of the eastern production fluids indicate that they are enriched in CO_2 relative to the western fluids. CO_2-enriched fluids are also preserved in fluid inclusions in GTW 3, but were not observed in GTW 5 or 6. These relationships suggest that the excess CO_2 is locally derived.

ACKNOWLEDGEMENTS

The authors would like to thank the management of Chevron Resources for enabling us to conduct this study and for providing the samples and well logs. We would also like to thank Bob Murray of Chevron Resources and the operations personnel at Heber. This research was supported by DOE contract DE-AC07-85ID12489.

REFERENCES

Browne, P. R. L., 1977, Occurrence and hydrothermal alteration of diabase, Heber geothermal field, Imperial Valley, California: Univ. Cal. Riverside, UCR/IGPP-77/9, 61 pp.

Fournier, R. O., 1981, Application of water geochemistry to geothermal exploration and reservoir engineering, in Rybach, L., and Muffler, L. J. P., eds., Geothermal Systems: Principles and Case Histories: John Wiley & Sons, New York, p. 109-143.

Fournier, R. O., and Truesdell, A. H., 1973, An empirical Na-K-Ca geothermometer for natural waters: Geochim. et Cosmochim. Acta, v. 37, p. 1255-1275.

James, E. D., Hoang, V. T., and Epperson, I. J., 1987, Structure, permeability and production characteristics of the Heber, California geothermal field: Proc. 12th Workshop on Geoth. Res. Eng., Stanford Univ., v. 12, p. 267-271.

Lippmann, M. J., and Bodvarsson, G. S., 1985, The Heber geothermal field, Califonia: natural state and exploitation modeling studies: Jour. Geophys. Research, v. 90, p. 745-758.

Potter, R. W., II, Clynne, M. A., and Brown, D. L., 1978, Freezing point depression of aqueous sodium chloride solutions: Econ. Geol., v. 73. p. 284-285.

Truesdell, A. H., Thompson, J. M., Coplen, T. B., Nehring, N. L., and Janik, C. J., 1981, The origin of the Cerro Prieto geothermal brine: Geothermics, v. 10, p. 225-238.

Tansev, E. O., and Wasserman, M. L., 1978, Modeling the Heber geothermal reservoir: Trans. Geotherm. Resour. Council, v. 2, p. 645-648.